Reactivation of schema representation in lateral occipital cortex supports successful memory encoding

Dingrong Guo[1], Jiongjiong Yang*

School of Psychological and Cognitive Sciences, Beijing Key Laboratory of Behaviour and Mental Health, Peking University, Beijing 100871, China

***Corresponding author:** Jiongjiong Yang, Ph.D., School of psychological and cognitive sciences, Peking University, Beijing 100871, P.R. China.

Telephone: 86-10-62766589; E-mail: yangjj@pku.edu.cn.

Running title: Cortical reactivations support schema memory

Conflict of interest statement: The authors declare no competing financial interests.

Acknowledgments: This work was supported by the grant from the National Natural Science Foundation of China [grant number: 32071027, J. Yang]. We thank Rik Henson for the comments/suggestions of the manuscript revision.

[1] Present address: MRC Cognition & Brain Sciences Unit, University of Cambridge, Cambridge, UK

Abstract

Schema provide a scaffold onto which we can integrate new memories. Previous research has investigated the brain activity and connectivity underlying schema-related memory formation. However, how schema are represented and reactivated in the brain, in order to enhance memory, remains unclear. To address this issue, we used an object-location spatial schema that was learned over multiple sessions, combined with similarity analyses of neural representations to investigate the reactivation of schema representations of object-location memories when a new object-scene association is learned. In addition, we investigated how this reactivation affects subsequent memory performance under different strengths of schema. We found that reactivation of a schema representation in the lateral occipital cortex (LOC) during object-scene encoding affected subsequent associative memory performance only in the schema-consistent condition, and increased functional connectivity between the LOC and parahippocampal place area. Taken together, our findings provide new insight into how schema acts as a scaffold to support the integration of novel information into existing cortical networks, and suggest a neural basis for schema-induced rapid cortical learning.

Keywords: schema; hippocampus; vmPFC; rapid cortical learning; representational similarity analysis.

Introduction

Our brains are able to incorporate new information into existing knowledge, which allows us to redefine and update our knowledge. For example, a professor might struggle to associate a group of students with their names at the very first class. After a few classes however, it becomes easier to remember the face-name associations because the professor has become familiar with the faces. Correspondingly, studies have shown that memory can be facilitated by information that we already know - namely, prior knowledge or schemas (van Kesteren et al. 2012; Gilboa and Marlatte 2017). The face-name associations will be even better remembered if the professor have more structural information about the students; for example, some students always sit at the same seats, or some students always sit together. This structural knowledge is the schema, which has been defined as abstract mental structures/neural networks that organize representations of our memories. In this case of building face-name associations, it may occur in two steps: First, the related structural memories of the students (e.g., seats and related faces) were reactivated; second, new memories were formed for the names that are associated with the faces. Although the effect of schema on memory encoding in humans is well documented (Gilboa and Marlatte 2017; Alonso et al. 2020), one important question remains unanswered: how the reactivation of schema representations helps to achieve memory integration and enhancement.

During schema-related memory formation, the schema support memory by providing an organisational framework within which we can encode and store relevant

information and efficiently incorporate new information (Bartlett 1932; Alba and Hasher 1983). Several previous animal (Tse et al. 2007; Tse et al. 2011; McKenzie et al. 2014; Baraduc et al. 2019; Zhou et al. 2021) and human (van Kesteren et al. 2013; van Kesteren et al. 2014; Brod et al. 2016; Liu et al. 2017; Bein et al. 2020; Nicolás et al. 2021; Tompary and Thompson-Schill 2021; Yousuf et al. 2021; Zheng et al. 2021) studies have investigated how schema or prior knowledge influence memory encoding. When incoming information can be directly linked to a pre-existing schema, the ventromedial prefrontal cortex (vmPFC) appears to be important for memory encoding (van Kesteren et al. 2010; van Kesteren et al. 2013; Giuliano et al. 2021). Specifically, vmPFC is believed to strengthen or weaken cortico-cortical functional connections (van Kesteren et al. 2013; Bein et al. 2020).

Another core brain region of schema-related processing is the hippocampus. However, involvement of the hippocampus during encoding is more complex and appears to be not only dependent on the schema-consistency of the new information but also on the characteristics of the schema to be encoded within. Animal studies show that the hippocampus is active during the encoding of schema-related updates, although schema-related memories can quickly become independent of the hippocampus (Tse et al. 2007; Baraduc et al. 2019). In human studies, on the one hand, studies have shown that hippocampal activity is increased when incoming information is schema-inconsistent (van Kesteren et al. 2013; Bein et al. 2014). On the other hand, using famous faces as schema, another study found that schemas facilitate the formation of

associative memory between faces and houses, and this process was related to enhanced activity in the hippocampus and its functional connectivity with the vmPFC (Liu et al. 2017). Similarly, van Kesteren et al. (2018) showed that the hippocampus is involved in translating previous spatial knowledge (i.e., a newly learned spatial schema) into new goal-directed behaviour. Furthermore, human lesion studies show that learning may occur in the absence of intact hippocampal structures if it is related to prior knowledge (Skotko et al. 2004; Ryan et al. 2020). In an fMRI study, repeated retrieval of a previously learned word list induced decreased hippocampal activity and increased cortical activity (Himmer et al. 2019), suggesting that activation of retrieval-induced prior representations may support cortical memory integration. Therefore, if the new information is encoded within a stable schematic structure, higher vmPFC activity and a greater number of cortico-cortical connections would be involved, with hippocampal engagement dependent on both the schema-consistency of the new information and the schema per se.

Although there are some exceptions (Brod et al. 2016; Sommer 2017), most human imaging studies on memory encoding use real-world schemas. These schemas include famous faces (Liu et al. 2017; Liu et al. 2018; Bein et al. 2019; Bein et al. 2020), semantically related word pairs (Bein et al. 2014), and congruent scene-object pairs (van Kesteren et al. 2013; Webb et al. 2016; Audrain and McAndrews 2022). However, due to the varied experiences of each individual, we cannot be sure of their precise schema, or how a specific schema reactivates during new learning. To extract the

specific schema representation, a schema that has been newly formed through training is required. Moreover, compared to univariate analysis, multivariate analysis can better address how schema reactivates during the new associative learning, and how a schema representation assimilates new information in brain regions.

In examining schema reactivation, one interesting theory from Bransford (1979) suggests that schemas are only effective in facilitating memory if they are activated from existing memory traces. Recent studies further show that the way in which schemas are expressed influences resultant memory formation (Masís-Obando et al. 2021; Tompary and Thompson-Schill 2021). At the behavioural level, reactivation of prior memories indexed by an individual's subjective score modulates subsequent memory performance (st. Jacques and Schacter, 2013; van Kesteren et al. 2018). At the neural level, studies using transitive inference (i.e., studying A-B and B-C, then inferring A-C) or narrative stimuli have shown that this reactivation is related to the activity of the hippocampus, particularly the anterior hippocampus (Schlichting et al. 2014; Schlichting et al. 2015; Baldassano et al. 2018; van Kesteren et al. 2020; Masís-Obando et al. 2021). One study further indicates that after associative learning of famous and novel face pairs, the neural representation of a novel face becomes similar to that of the famous face in inferior frontal gyrus, suggesting the cortical assimilation of new information into old memories (Bein et al. 2020). In addition, memory reactivation in cortical regions is a central component of computational theories of memory (McClelland 2013; McClelland et al. 2020), which hold that reactivation

supports the stabilisation of memory over distributed brain networks. Schemas may also enhance rapid integration of new information into existing cortical neural networks (Hebscher et al. 2019). Thus, we propose that schema reactivation in relevant cortical regions (relevant to the specific stimulus material), and the interaction of this reactivation with new information, are important for successful schema-related memory encoding.

In sum, the main objective of the study was to to use an experimentally learned spatial schema and neural representational similarity analyses in order to determine the neural basis of schema representations in new learning and how the representations affected subsequent memory. The present study expands on our prior work (Guo and Yang 2020), in which participants spent three days in the training session over-learning four grids: two schema-consistent (schema-C) grids and two schema-inconsistent (schema-IC) grids. Each grid contained a number of object-location trained pair associations (PAs) that form a spatial schema. On the schema-C grids, the objects and locations of the trained PAs on each grid were repeated consistently across days 1-3, while the combinations on the schema-IC grids changed across days. Therefore, the objects in the schema-C condition were always presented in a stable context and should form a schema, while the objects in the schema-IC condition should not have a stable structure (and no or only a weak schema). In the new learning session, the participants first retrieved the object-location associations (e.g., schema elements/representations, Phase 1), before learning new object-scene associations (Phase 2) in an fMRI scanner

(on Day 4). Associative memory was then tested outside the scanner on Day 5. Here we also report results from a behavioural pilot experiment, used to explore the schema effects in two different memory tests at two different delays. Previous studies (Hennies et al. 2016; Bonasia et al. 2018; Guo and Yang 2020; Audrain and McAndrews 2022), and results of the behavioural pilot experiment, show that schema effects are strongest after a delay. Based on that, a single delayed associative memory test was used in the fMRI experiment, which also better matched the trial numbers between remembered and forgotten trials in the fMRI analyses.

In the fMRI univariate analysis, we focused on the vmPFC and hippocampus, given the evidence reviewed above that their activations are critical for schema-related memory encoding (Preston and Eichenbaum 2013; Gilboa and Marlatte 2017; Robin and Moscovitch 2017). In terms of the hippocampus, the anterior portion seems to be the most involved in schema-related memory integration (Schlichting et al. 2015; van Kesteren et al. 2020; Masís-Obando et al. 2021) and spatial schema processing (Audrain and McAndrews, 2022; Guo and Yang, 2020). Furthermore, in the multivariate analysis, we focused on stimuli-relevant cortical regions and sought to investigate how reactivation of representations of previously-formed schema helps memory integration through two steps:

First, to examine whether object-location retrieval in the same grid contains shared representation of grid-based information (i.e. schema information), and whether objects presented during associative learning also represent a similar grid-based

representation, we compared neural similarity 1) when participants retrieved object–location memories from the same versus different grids during Phase 1; 2) when they learned the new object–scene associations in which the objects were from the same versus different grids during Phase 2. The neocortical regions that support lasting memory representations include brain areas involved in the original processing of the stimulus at the time of encoding (Tulving and Thomson 1973; Nyberg et al. 2000; Danker and Anderson 2010). Given that the schema involved visual objects, the ventral visual area of the lateral occipital cortex (LOC) was a third region of interest (ROI), which was also a main ROI in the multivariate analysis. The LOC is activated by pictures of objects with categorical consistency (Eger et al. 2008) and this response respects categorical similarity (Bracci and de Beeck 2016). This region also plays an important role in object-based schema formation (van der Linden et al. 2017). Therefore, we expected the LOC would contain the grid (schema)-based information.

Second, to investigate how schematic representation (Phase 1) reactivates during new associative learning (Phase 2) and affects subsequent memory performance (Phase 3), we measured the similarity between object–location memory retrieval and associative learning of the same object, as well as its relationship with subsequent memory. We postulated that the neural reactivation of prior object-location memory in the LOC would enhance subsequent memory under the schema-C condition. A final ROI was the parahippocampal place area (PPA), given prior evidence that this region is involved in processing spatial layouts (Epstein and Baker 2019). As schemas induce

the formation of cortico-cortical connections (van Kesteren et al. 2014; Liu et al. 2017), the LOC and PPA might be more strongly connected when an association is subsequently remembered in the schema-C condition.

Materials and methods

Participants

A total of 49 participants were recruited from the Peking University community and were paid for their participation. Of these, 24 were tested in the behavioural pilot and the remaining 25 were test with fMRI. The data of the behavioural pilot were collected in order to optimize the design of the fMRI study. Therefore, for full counterbalancing across schema conditions, 24 participants were recruited for the behavioural pilot. However, one of them quit after the 3-day training, leaving 23 with data (15 female; mean age = 20.35 years, SD = 1.75). For the fMRI study, we aimed to have a similar number of participants. Because one participant had a low response rate (70/120) in the scanner, we replaced them, leaving a fully counterbalanced 24 participants (15 female; mean age = 20.67 years, SD = 2.01) in the final fMRI group. All participants were native Chinese speakers and gave written informed consent in accordance with procedures and protocols approved by the department Review Board of Peking University.

Materials

In our previous study (Guo and Yang, 2020), layouts of object–location PAs were used to manipulate schema. The manipulation of schema was similar in this study; however, to induce better representations of the objects in the cortical region (i.e., the LOC), colour pictures of objects were used instead of grayscale pictures (Figure 1A).

Figure 1. Experimental procedure and behavioural results of the fMRI group. **(A).** Procedure. During the initial three-day training session, two schema-C grids and two schema-IC grids with different-coloured backgrounds were trained. During the new learning session, Phases 1 and 2 took place on Day 4; Phase 1 was an object–location retrieval task involving the trained pair associations, while Phase 2 was an object–scene association task where participants were asked to imagine the object in the scene vividly and then judge whether this was easy or not easy. Phase 3, which occurred on Day 5, was a memory test in which object–scene memory was tested. **(B).** Behavioural results. The left panel illustrates memory performance for each schema

condition during the training session (cycle = c1, c2, c3; day = D1, D2, D3). Error bars represent the standard error of the mean (SEM). The right panel illustrates memory performance during the new learning session. Box plots display the minimum, first quartile, median, third quartile, and maximum (bottom to top) of the data. Points represent individual participants and grey lines represent the schema-C to schema-IC trend for each participant.

In the new learning session, for the fMRI group, 120 object–scene pairs were used. The 120 objects (see description of training session below) had been learned in either the schema-C or schema-IC condition during the training session. The 120 scenes were selected from our previous study (Zhan et al. 2018) and divided into four groups of 30 scenes. The four groups of scenes had similar levels of familiarity and visual complexity (all $F < 1$, $p > 0.7$). They were then randomly paired with four groups of object pictures. The assignment was counterbalanced across participants and schema conditions. Therefore, the associative task included 120 object-scene pairs, 60 of which included objects learned in the schema-C condition and 60 of which included objects learned in the schema-IC condition. In the following object-cued associative memory test, participants were shown an object together with four scenes; of these scenes, one had been presented with the object during the encoding phase (target), whereas the other three were scenes seen with other objects during encoding (lures). To reduce the interference between different grids, the objects paired with lures and the object paired

with the target were from the same grid during the training session. The possible positions of the target were counterbalanced across trials and participants.

For the behavioural pilot group, in addition to the 120 scenes above, another 120 scenes were selected in the same way, and also divided into four groups of 30 scenes. Tests of both item memory for the scenes and associative memory for the object-scene pairing were conducted immediately and 24-hours later. Therefore, half of the old scenes and half of the new scenes in each condition were randomly used for the item memory tests at each test delay. The corresponding object-scene associative memory test was conducted after the item memory test.

For the schema training session, 120 colour pictures of everyday objects were selected from a bank of standardized stimuli (Brodeur et al. 2010) and the internet. In a previous study, 25 participants (14 female; mean age = 21.52 years, SD = 2.12) were asked to name the objects in question and rate the pictures for their familiarity and object agreement (Brodeur et al. 2010; Moreno-Martínez and Montoro 2012). The naming accuracy for each object was calculated as the proportion of participants who correctly named the object. Rating scores (i.e., familiarity and object agreement) ranged from 1 (lowest) to 7 (highest). The final 120 pictures selected for this study were easy to name (0.73 ± 0.28) and had high levels of familiarity (5.51 ± 1.11) and object agreement (5.93 ± 0.47).

Similar to our previous study (Guo and Yang, 2020), four grids were used for the schema-C and schema-IC conditions and the pictures were divided into four object

sets with 30 pictures for each grid. The four object sets were comparable in terms of naming accuracy, familiarity, and object agreement (all $F < 1$, $p > 0.8$). They were also matched for category, colour, and size and assigned to different schema conditions. The assignment was counterbalanced across participants. The locations used in this study were situated on four 8×8 grids, which differed only in the colours of their backgrounds (i.e., red, yellow, blue, and green). Two grids were used for each schema condition. Assignment of grid colours to the schema-C and schema-IC conditions was counterbalanced over the participants. Then four location sets of 30 locations each were created and assigned to different schema conditions. This assignment was also counterbalanced across participants. The locations within each pair of location sets were selected in such a way that the 60 locations (60 of 64 possible locations excluding the locations of the four corners) of a grid were pseudo-randomly assigned in two sets of 30 locations, and the locations of each set were distributed evenly over the four quadrants of the grid (seven or eight on each quadrant). Then, the 30 objects contained in a specific object set were pseudo-randomly assigned to the 30 locations of its corresponding location set. This resulted in two schema-C grids and two schema-IC grids, with each grid consisting of 30 PAs. On each grid, all 30 PAs were overlearned as the trained PAs in the training session (this occurred differently for the schema-C and schema-IC conditions; see below).

The schema-C and schema-IC grids differed in the consistency of the trained PAs across the days of the training session. On each schema-C grid, the 30 trained PAs

remained unchanged and were consistent from day 1 to day 3. On each schema-IC grid, the objects and possible locations of the 30 trained PAs were fixed but the combinations between them changed across the training days (although they remained consistent within the same day). Therefore, on day 4, half of the objects had a prior stable schema structure that could be integrated during the new learning stage, and the other half had no such structure.

Procedure

The experiment was divided into two sessions: a training session and a new learning session (Figure 1A). The training session occurred over the first three days. During this session, participants were trained to learn four grids of 30 object–location PAs. The new learning session was performed on Days 4 and 5. On Day 4, the participants retrieved trained PAs and learned 120 scene–object associations (these tasks were performed inside the scanner for the fMRI group). In the behavioural pilot group, both item memory and scene–object associative memory were tested immediately, as well as on Day 5. In the fMRI group, the scene-object associative memory was only tested on Day 5, outside of the scanner.

The first two days of the training session involved three learning-test cycles, and the PAs in each grid were learned and tested with feedback once per cycle. This procedure was similar to that used in our previous study (Guo and Yang, 2020); however, because there were more PAs in each grid in the present study, the grid was

presented on the screen for 120 s rather than 90 s at the start of each cycle. The two grids for the same schema condition were always trained successively, and their order was counterbalanced across the days and participants.

The procedure for the third day also involved three cycles. To obtain a final measure of training performance, the two grids for one of the schema conditions were trained again successively at the end of the usual training cycle, followed by a 5 min odd/even digit task and retrieval task without feedback (see description of tasks in the new learning session). Then, the remaining two grids for the other schema condition were trained and tested using the same procedure. The presentation order of the 30 object cues for each grid was randomized and varied across cycles and days. The order of the schema conditions was counterbalanced across cycles, days, and participants.

For the fMRI group, the new learning session consisted of three phases for each condition (schema-C, schema-IC): a retrieval task for the trained PAs (Phase 1, not applicable in the behavioural group), an associative learning task focused on object–scene association (Phase 2), and a memory test for object–scene association (Phase 3). Phase 1 involved two runs of the retrieval task, each consisting of 60 trials and lasting about 9 min. During the task, the tested grids alternated every five trials. At the beginning of every five trials, a coloured grid corresponding to one of the schema-C or -IC grids was first shown on the screen for 4 s. For each trial, a randomly selected object cue was presented in the centre of the screen for 1 s, then participants moved the cursor and pressed the left button of the mouse to select the correct location on the grid within

a response period of 3 s. After the selection, the grid turned grey and feedback was no longer presented. Before the next trial, a "+" was shown on the screen for 2 s. After the five trials were complete, a blank screen appeared for 10 s to reduce neural interference between the different grids. The order of the schema conditions was counterbalanced across participants.

The associative encoding task (Phase 2) also involved two runs, each consisting of 60 trials and lasting about 9 min. During the object–scene associative task, successive objects were from the same grid and alternated between grids every five trials. At the beginning of every five trials, a coloured grid corresponding to one of the schema-C or -IC grids was first shown on the screen for 4s. For each trial, an object–scene image pair was presented for 3s, with the object on the left of the screen, the scene on the right, and a "+" in between. Participants were required to look at the object–scene pairs and imagine as vividly as possible that the object was in the scene. While the pictures were still on the screen, the words "Easy" and "Not easy" appeared at the bottom for 1s; participants needed to press one of two buttons to indicate whether it was easy or not easy to imagine the object–scene pair in this period. After the five trials were complete, a blank screen appeared for 10s to reduce neural interference between the different grids. The order of schema conditions was counterbalanced across participants. After the associative encoding task, a 10 min structural scan was performed. The total scanning time was approximately 1 h.

The memory test was performed on day 5; here, the 120 object–scene associations that were learned on day 4 were tested. Participants were cued with all 120 objects again in a pseudo-random order. They were given four scenes for each object; one of these had been presented with the object during the encoding (target), whereas the other three were scenes seen with other objects during encoding (lures). Participants indicated their choice by pressing the appropriate button. Afterwards, they were asked to rate their level of confidence in their decision on a scale of 1 (not sure) to 4 (very sure). They were given no time limit for their responses but were told to answer as quickly and honestly as possible. The testing procedure was similar in the behavioural group, except half of the object–scene associations were tested on day 4 and the other half were tested on day 5.

In addition, for the behavioural pilot group, item memory tests were conducted immediately and 24-hour later. During the test, the old or new scene was presented at the centre of the screen, and the participants made a self-paced judgement of whether or not they had seen the scenes during the learning phase. If the scene was judged as "old", the participants were asked to make self-paced remember/know/guess judgement (Rajaram 1993; Gardiner et al. 1998).

fMRI data acquisition

A 3T Siemens Prisma MRI scanner with a 20-channel head coil in the MRI Center at Peking University was used to acquire MRI images. In the structural MRI

scan, T1-weighted high-resolution MRI volumes were obtained using a 3-dimensional magnetization-prepared rapid acquisition gradient echo (MPRAGE) sequence (FOV = 256 × 256 mm; matrix = 256 × 256; slice thickness = 1 mm, TE/ TR = 2.98/2530 ms, flip angle = 7°). High-resolution functional MRI image were obtained using a simultaneous multiband EPI sequence (FOV = 224× 224 mm; matrix = 112 × 112, resolution = 2 ×2 × 2 mm, TE/ TR = 30/2000 ms, flip angle = 90°). Visual stimuli were presented using MATLAB 2014b (MathWorks, Natick, MA, USA) and elements of the Psycholotoolbox3 (Brainard and Vision 1997; Pelli 1997; Kleiner et al. 2007), back-projected to a screen, and viewed with a mirror mounted on the head coil. Responses were collected with an MRI-compatible mouse.

fMRI analyses

The AFNI software package (Cox 1996) was applied for the fMRI preprocessing. The first 6 volumes of the EPI images were removed to allow for scanner stabilization. EPIs were corrected for motion (3dvolreg) and slice timing (3dTshift), masked to exclude voxels outside the brain (3dautomask), and were smoothed (3dmerge) using a 2.0mm Gaussian FWHM kernel. Each run was also despiked to further reduce the influence of motion on the data (3dDespike). Functional scans were aligned to each subject's skull-stripped MP-RAGE (align_epi_anat.py).

Pre-processed scans were modelled in each subject's native space. A least-squares single (LSS) pattern estimation approach (Mumford et al. 2012; Mumford et al.

2014), was used to estimate each trial's activation at every voxel ("beta map"). These steps were performed in AFNI using 3dDeconvolve. Six regressors were used to capture motion. In the general linear model (GLM), deconvolution of the hemodynamic response was done using tent functions spanning a period of 32 s after the onset of the first of every five trials, with 17 estimator functions distributed across this time window.

As in our previous study (Guo and Yang, 2020), we defined the vmPFC and hippocampus anatomically; anatomical masks of each side of the hippocampus were created using AFNI's FS_Desai_PM atlas, which was originally parcellated using FreeSurfer (Fischl and Dale 2000). The anterior hippocampus was defined as $y > -21$ in Talairach space (Poppenk et al. 2013; Guo and Yang 2020). The vmPFC anatomical mask was first defined using the Mackey vmPFC Atlas (Mackey and Petrides 2014), then was further defined as the 14m subregion in this mask following Guo and Yang (2020). We then defined ROIs for object processing (LOC) and scene processing (PPA). The LOC was defined bilaterally using AFNI's CA_N27_ML atlas, while the PPA was defined based on our previous study (Zhan et al. 2018). As all analyses were performed in the subjects' native space, the ROIs were transformed into each participant's space using AFNI's 3dAllineate program.

For all analyses described below, we used the mean beta map for the period 4-8 s after the onset of each trial, i.e., the mean value of the 3rd and 4th estimated beta parameters after the onset of each trial from the output of 3dDeconvolve. These beta values were used in conjunction with the ROIs to perform several analyses: 1. to assess

the effect of brain activation on subsequent memory, we first performed a univariate analysis in the regions of interest. 2. To examine the effects of schema reactivation and brain connectivity on memory, we then performed separate representational similarity analyses and beta series correlation analyses. In addition, in a trial-based analysis, we found that 5 of 120 trials had lower overall memory performance than the performance by randomly guessing (i.e., less than 25% of participants (6/24) responded correctly on these trials in the final test), we therefore only analysed the remaining 115 trials in all the fMRI analyses.

Univariate ROI analysis

We mainly utilized multivariate analyses in this study. However, to compare our results with those of previous studies that used univariate analysis, we also performed univariate ROI analysis. In the univariate analysis, to replicate the results of previous studies, we mainly focused on the results in the vmPFC and aHPC. Then, we also performed an exploratory univariate analysis in the ROI (LOC) of multivariate analysis (see supplementary material). For each ROI, the mean activation of a condition was calculated by averaging all the betas (for each trial) across voxels within each ROI and across trials within each condition. During the retrieval of trained PAs (phase 1), only correct trials were included in the analysis. Because there were too few trials (< 9) for at least one condition in three participants, this analysis included only 21 participants. Differences between the subject-averaged beta-weights were investigated using paired

two-tailed t-tests with a threshold of $p < 0.05$. A 2×2 repeated-measures ANOVA was then performed on the data from associative encoding (Phase 2) with factors of schema (schema-C, schema-IC) and memory (remember, forget). This analysis included all 24 participants.

Representational similarity analysis (RSA)

Our main hypothesis asks whether the LOC contains schematic representations, and how reactivation of these affects subsequent associative memory. To test this, an RSA was conducted on beta maps generated from data in the subjects' native space. Voxel-wise patterns of hemodynamic activity were separately extracted for each hemisphere of LOC from the single trial beta maps. First, we wanted to know whether LOC carried schema-related information, which was grid-based in our study. To test this, we compared the within-grid and across-grid similarity for each ROI. In each phase (Phases 1 and 2), within-grid similarity was calculated as the Pearson correlation of the betas between an object and 'all other objects' in the same grid. To reduce effects of temporal autocorrelation, within-grid similarities between trials that were within the set of 5 consecutive positions (grids alternated every five trials during both Phase 1 and Phase 2) were excluded. Across-grid similarity was calculated as the Pearson correlation of the betas between an object and all objects in the other three grids. All correlations were Fisher-transformed prior to statistical testing. We then performed a paired t-test to compare the mean values of within-grid and across-grid similarity.

During the retrieval of trained PAs (phase 1), only correct trials were included in the analysis. Because there were too few trials (< 9) for one of the conditions in three participants, this analysis included 21 participants. During associative encoding (Phase 2), only subsequently remembered trials were included in the analysis. This analysis included all 24 participants.

For the schema reactivation in the LOC, it was calculated as the Pearson correlation of the betas between the two phases of object presentation in the retrieval of training PAs (Phase 1) and new learning of object–scene associations (Phase 2). Values were Fisher-transformed prior to statistical testing. Then, a schema (schema-C, schema-IC) × memory (remember, forget) ANOVA was performed to test how reactivations of schematic information were related to subsequent memory under different schema conditions. To explore the potential effects in the ROIs (vmPFC and aHPC) of univariate analysis, same representational similarity analyses were then also performed in these regions (see supplementary material).

Beta series correlation (BSC) analysis

Another hypothesis concerns the connectivity between the LOC and PPA. Because we used a trial-based GLM, a beta series correlation (BSC) analysis was conducted to measure brain connectivity (Rissman et al. 2004). In this analysis, the betas were averaged across voxels within the ROI for each trial. The connectivity between two ROIs under can then be quantified by calculating the Pearson correlation

coefficient across trials for each condition. Correlation coefficients were Fisher-transformed prior to statistical testing. Using a paired *t*-test, we directly compared LOC–PPA connectivity for subsequently remembered trials between the two schema conditions.

Results

Behavioural results

For the associative memory test, the memory performance was measured by the rate of correct trials as well as the rate of high confidence (confidence >= 3) correct trials. For the item memory test, the memory performance was measured by hit rate and also by splitting it into recollection and familiarity based on the remember/know/guess judgement (Yonelinas 2002). The behavioural results are shown in Figure 1B, and analysed below.

Behavioural pilot group

For the training phase, consistent with our previous study (Guo and Yang 2020), participants showed a significant schema effect in the final test on day 3 (0.90 ± 0.10 vs. 0.70 ± 0.15; $t\,(22) = 6.22$, $p < 0.001$), suggesting a successful training of schema.

During the associative encoding phase of the new learning session, participants reported that object–scene pairs were easier to imagine in the schema-C condition than

the schema-IC condition (proportion of easy: 0.48 ± 0.10 vs. 0.45 ± 0.11, t (22) = 2.49, p = 0.020, Cohen's d = 0.52).

For the hit rate of the item memory test in the new learning session, no interaction or main effect of schema was found in the schema × test delay ANOVA (all p > 0.23). Further, to explore the schema effects in different test delay, two separate paired t-test were performed. Neither immediate test (0.77 ± 0.14 vs. 0.77 ± 0.15, t (22) = 0.12, p = 0.904, Cohen's d = 0.03), nor 24-hour test (0.54 ± 0.20 vs. 0.57 ± 0.15, t (22) = 1.12, p = 0.274, Cohen's d = 0.23), showed significant schema effect. When splitting item memory into recollection and familiarity, neither showed a schema effect in either of the test delays (all p > 0.39).

For the associative memory test, no interaction was shown in the schema × test delay ANOVA (F (22) = 1.044, p = 0.318, η^2 = 0.003), but the main effect of schema approached significance (F (22) = 3.922, p = 0.060, η^2 = 0.018). In order to find best delay for fMRI experiment, paired t-test was performed separately at each test delay. The results showed a significant schema effect for the test after 24 h (0.65 ± 0.11 vs. 0.60 ± 0.13, t (22) = 2.62, p = 0.016, Cohen's d = 0.55; high confidence (confidence >= 3): 0.65 ± 0.11 vs. 0.64 ± 0.17, t (22) = 1.487, p = 0.151, Cohen's d = 0.31), but not for the immediate test (0.84 ± 0.09 vs. 0.82 ± 0.13, t (22) = 0.766, p = 0.452, Cohen's d = 0.16; high confidence (confidence >= 3): 0.38 ± 0.17 vs. 0.34 ± 0.17, t (22) = 1.487, p = 0.873, Cohen's d = 0.03).

Because the pilot showed that schema seem to exert a stronger effect on associative than item memory, and for delayed relative to immediate test, we restricted the fMRI experiment to a delayed test of associative memory, which also better matched the trial numbers between remembered and forgotten trials for fMRI analyses.

fMRI group

In the fMRI group, the results also showed a significant schema effect of training in the final test on Day 3 (0.90 ± 0.11 vs. 0.65 ± 0.11; t (23) = 6.04, $p < 0.001$; Figure 1B). This schema effect was maintained in the retrieval task during the new learning session on Day 4 (0.81 ± 0.14 vs. 0.47 ± 0.22; t (23) = 15.02, $p < 0.001$).

For the easy of imagery judgement in the associative encoding phase of the new learning session, any difference between the two schema conditions did not reach significance (proportion of easy: 0.52 ± 0.16 vs. 0.53 ± 0.17, t (23) = 0.28, p = 0.784, Cohen's d = 0.06), unlike the behavioural pilot. For the associative memory test, although the memory performance was numerally higher in the schema-C condition than in the schema-IC condition, no significant difference was found between the two schema conditions (0.48 ± 0.13 vs. 0.47 ± 0.12, t (23) = 0.964, p = 0.345, Cohen's d = 0.20; high confidence: 0.26 ± 0.18 vs. 0.24 ± 0.14, t (23) = 1.21, p = 0.238, Cohen's d = 0.25; Figure 1B).

To better clarify behavioural patterns and increase the statistical power, we combined the data for the two groups. These results showed a similar trend to that of

the behavioural group during associative encoding: there was no significant difference in the proportion of easily imagined object–scene pairs between the two conditions during memory encoding (proportion of easy: 0.50 ± 0.14 vs. 0.49 ± 0.15, t (23) = 1.37, p = 0.183, Cohen's d = 0.03), but there was a significant schema effect for associative memory 24 h later (0.57 ± 0.15 vs. 0.54 ± 0.14, t (46) = 2.66, p = 0.011, Cohen's d = 0.39; high confidence: 0.32 ± 0.18 vs. 0.29 ± 0.16, t (46) = 1.93, p = 0.059, Cohen's d = 0.28) .

fMRI results

Activations in the anterior hippocampus and vmPFC

During the retrieval of trained PAs (Phase 1), greater activation for correct trials in the schema-C than schema-IC condition was seen in both sides of the vmPFC (left: t (20) = 2.86, p = 0.009, Cohen's d = 0.61; right: t (20) = 3.29, p = 0.003, Cohen's d = 0.70; Figure 2A) and in the right aHPC (t (20) = 2.62, p = 0.016, Cohen's d = 0.56; Figure 2A). This was consistent with our previous results reporting schema-related activations in the vmPFC and right anterior hippocampus for trained PAs (Guo and Yang, 2020). The left anterior hippocampus showed the same trend, but did not reach significance (t (20) = 1.39, p = 0.18, Cohen's d = 0.62).

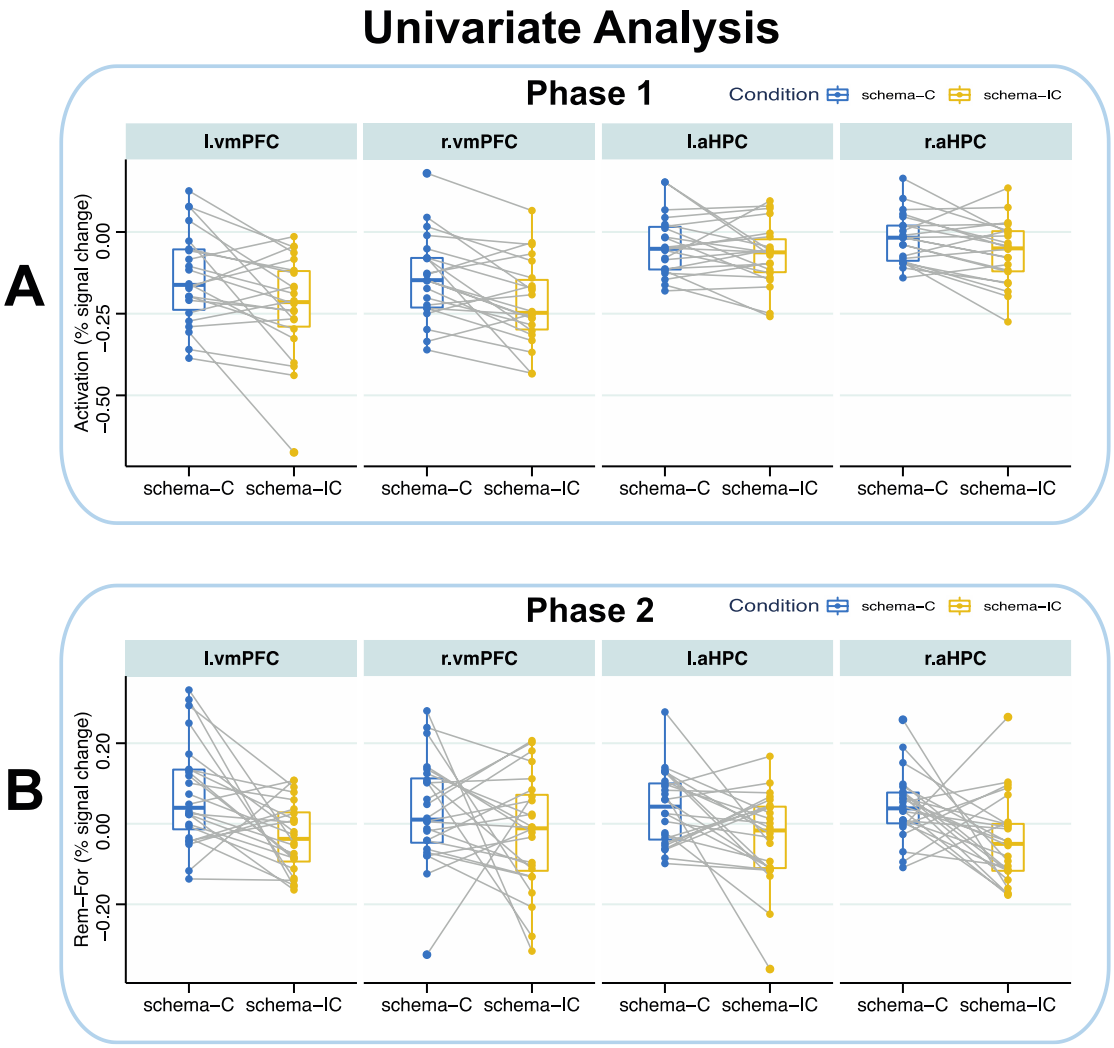

Figure 2. Brain activations of the vmPFC and anterior hippocampus during Phase 1 and Phase 2. (A) Activations of correct trials in different conditions. (B) Subsequent memory effect (Remember vs. Forget) in different conditions. Box plots display the minimum, first quartile, median, third quartile, and maximum (bottom to top) of the data. Points represent individual participants and grey lines represent the schema-C to schema-IC trend for each participant.

For associative encoding (Phase 2), the schema × memory ANOVA showed the critical significant schema by memory interaction in the left vmPFC (F (1,23) = 10.922, p = 0.003, η^2 = 0.32) and both sides of the aHPC (left: F (1,23) = 6.032, p =

0.022, η^2 = 0.21; right: F (1,23) = 6.582, p = 0.017, η^2 = 0.22). The right vmPFC (F (1,23) = 1.53, p = 0.229) showed a similar trend. Further pairwise analysis revealed that each of the three regions exhibited a significant subsequent memory effect in the schema-C condition (left vmPFC: t (23) = 2.80, p = 0.01, Cohen's d = 0.57; left aHPC: t (23) = 2.08, p = 0.049, Cohen's d = 0.43; right aHPC: t (23) = 2.51, p = 0.02, Cohen's d = 0.51; Figure 2B) but not in the schema-IC condition. This suggests that activations in the vmPFC and anterior hippocampus are vital for new associative encoding in schema-related networks. We also performed same analyses of activation in the LOC during Phases 1 and 2 (Figure S1). However, no significant effect of schema was detected in those regions.

Schema representations

During the retrieval of trained PAs (Phase 1), greater within-grid than across-grid similarity for correct trials was found in the LOC (left: t (20) = 3.79, p = 0.001, Cohen's d = 0.83; right: t (20) = 2.47, p = 0.023, Cohen's d = 0.54; Figure 3A). This was consistent with our hypothesis that the LOC should represent schemas during retrieval of trained PAs. Analyses also showed greater within-grid than across-grid similarity for correct trials in both sides of the vmPFC (left: t (20) = 2.864, p = 0.016, Cohen's d = 0.58; right: t (20) = 3.00, p = 0.007, Cohen's d = 0.66; Figure S2), left anterior hippocampus (t (20) = 2.72, p = 0.013, Cohen's d = 0.59; marginally significant on the right side: t (20) = 1.92, p = 0.069, Cohen's d = 0.42; Figure S2).

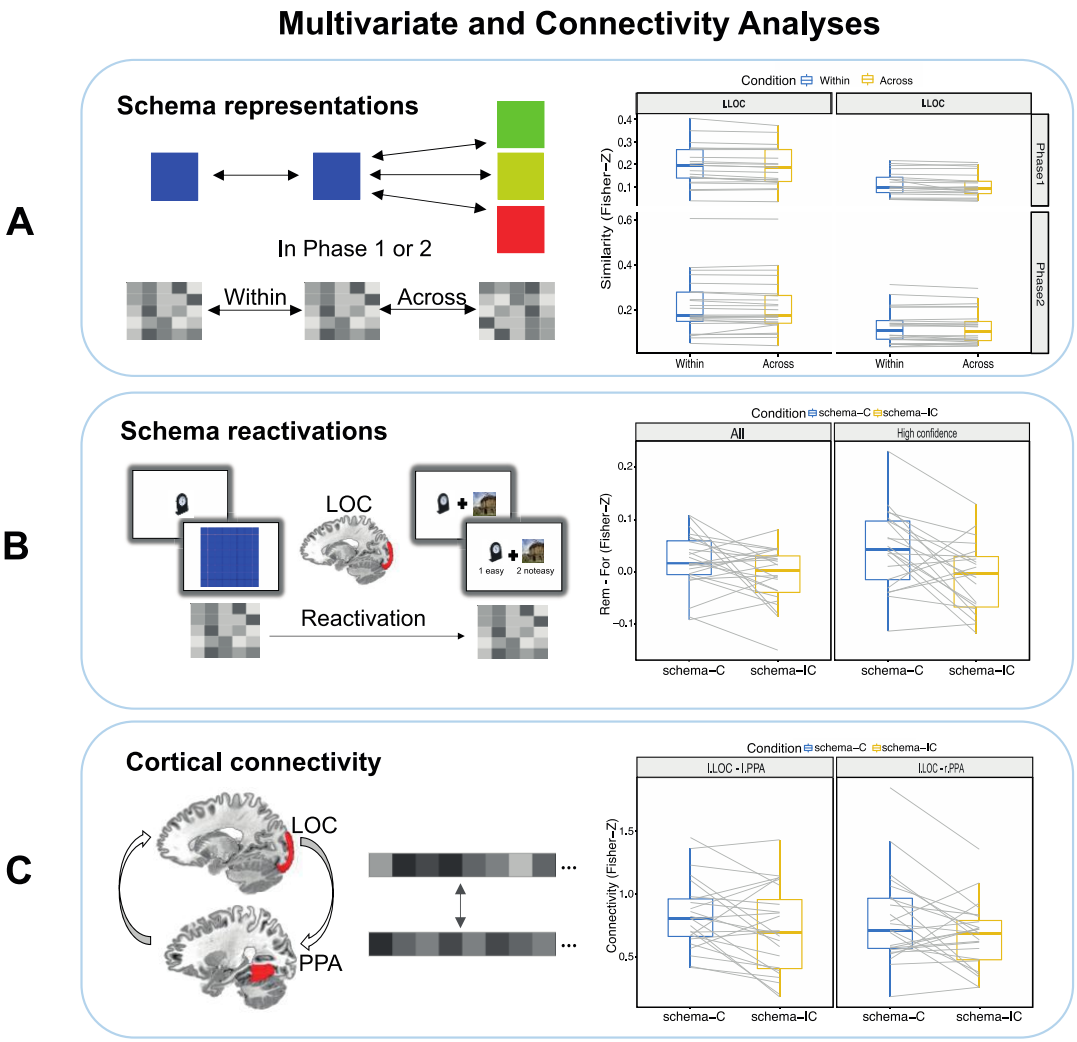

Figure 3. Results of multivariate analysis and connectivity analysis. **(A).** Within- and across-grid similarity for left and right LOC in Phases 1 and 2. **(B).** Effect of pattern reactivation (reactivation of patterns learned in phase 1 during phase 2) on subsequent memory (Remember -Forget). **(C).** Beta series correlations (brain connectivity) between the LOC and PPA. Points represent individual participants and grey lines represent the within- to across-grid similarity trend (on A) or schema-C to schema-IC trend (on B and C) of each participant. All the box plots display the minimum, first quartile, median, third quartile, and maximum (bottom to top) of the data.

For associative encoding (Phase 2), no strong difference was shown between within-grid than across-grid similarity for subsequently remembered trials in the LOC (left: t (23) = 0.56, p = 0.584, Cohen's d = 0.11; right: t (23) = 2.14, p = 0.043, Cohen's d = 0.44; Figure 3A). In the exploratory analyses, significant difference was seen in the anterior hippocampus (left: t (23) = 2.86, p = 0.010, Cohen's d = 0.57; right: t (23) = 2.85, p = 0.009, Cohen's d = 0.58; Figure S2), but not in the vmPFC (left: t (23) = 1.90, p = 0.070, Cohen's d = 0.39; right: t (23) = 1.95, p = 0.064, Cohen's d = 0.40; Figure S2). Results here suggest that the LOC may not carry general schematic representations during associative encoding, but are still possibly associated with successful assimilation of new information into such schemas (schema representations were clearly shown in the left LOC during Phase 1).

Cortical reactivation of schema representations during new associative learning

As our main hypothesis, we tested whether the reactivation of patterns learned in phase 1 during phase 2 was related to memory performance. There was a significant interaction between schema condition and memory in the left LOC (F (1, 23) = 4.254, p = 0.051, η^2 = 0.16, Figure 3B), but not in the right LOC (F (1,23) = 2.05, p = 0.166). Further analysis showed that the interaction was due to a significant subsequent memory effect in the schema-C condition but not the schema-IC condition. Next, we performed the same analysis using the high-confidence remembered trials. These results also showed a significant interaction between schema condition and memory in

the left LOC (F (1, 20) = 8.898, p = 0.007, η^2 = 0.31, Figure 3B), but not in the right LOC (F (1,20) = 1.595, p = 0.221, η^2 = 0.31). The interaction was again due to a significant subsequent memory effect in the schema-C but not the schema-IC condition. The reactivation results in left LOC were consistent with the last part that the left LOC had a greater within-grid than across-grid similarity during Phase 1. These results suggest that the reactivation of schematic information in the LOC facilitates the successful encoding of associative memory in the schema-C condition. We conducted similar analyses on the other ROIs, including the aHPC and vmPFC; however, no significant memory effects were detected in these regions (Figure S3).

Connectivity between the LOC and PPA in new associative learning

Our second hypothesis was that pattern reactivation could induce the formation of direct cortical connections. We tested this hypothesis using beta series correlation (BSC). Because reactivation was observed only in the left LOC, we calculated the BSC between the left LOC and both sides of the PPA. We selected the remembered trials for the two schema conditions. Both left LOC–left PPA connectivity and left LOC–right PPA connectivity exhibited greater BSC in the schema-C condition than in the schema-IC condition (left PPA: t (23) = 2.18, p = 0.040, Cohen's d = 0.44; right PPA: t (23) = 2.06, p = 0.050, Cohen's d = 0.42; Figure 3C). The results suggest that reactivation in the LOC might induce a direct LOC–PPA connection.

Discussion

The primary objective of this study was to determine the neural basis of schema representations and how the reactivation of schema representations affected subsequent memory. Our behavioural pilot showed that a consistent schema improved associative memory on a 24-hour delayed test. Though this schema effect on behavioural data did not reach significance in the fMRI group, the fMRI data showed clear differences in brain activation, multivoxel patterns and trial-wise connectivity between the two schema conditions. More specifically, we found that grid-based schematic information was represented in the LOC during the retrieval of trained PAs, but was not obvious during new associative encoding. However, the reactivation of grid-based representations in the LOC had a significant effect on subsequent memory in the schema-C condition, and increased LOC–PPA functional connectivity. In addition, activations in the vmPFC and anterior hippocampus were associated with successful new associative encoding. These results are consistent with our hypothesis that the reactivation of schema in the cortex is important for schema-related learning.

In the current study, we utilized a human analogue of training spatial schema first developed in van Buuren and colleagues (2014), which was similar to those used in classical rodent studies (Tse et al. 2007; Tse et al. 2011). This allowed us to better extract specific grid-based schema representations during the retrieval of training pair associations, as well as further measure reactivation and its relation to memory performance. Consistent with previous findings (e.g., Tse et al., 2007, 2011; Audrain

and McAndrews 2022; Guo and Yang 2020), our univariate analysis showed that the vmPFC and anterior hippocampus were involved in schema-related retrieval and new associative encoding. The vmPFC is known to be intensively involved in schema processing (Tse et al. 2011; Gilboa and Marlatte 2017). The anterior hippocampus has also been associated with schema-based memory integration (Schlichting et al. 2014; Schlichting et al. 2015; van Kesteren et al. 2018; Masís-Obando et al. 2021), and encoding of the overlapping information is associated with increased functional coupling between the vmPFC and anterior hippocampus (Zeithamova and Preston 2010; Zeithamova et al. 2012). Therefore, our results concerning brain activation further confirm that activity in the vmPFC and anterior hippocampus is important in schema-based associative integration (Audrain and McAndrews 2022; Guo and Yang 2020). This is also consistent with the view that the vmPFC and aHPC represent schema and gist information respectively (Robin and Moscovitch 2017; Sekeres et al. 2018).

Through neural representational similarity analyses, we saw that although the LOC carried schematic information (i.e., within > across) mainly in Phase 1, neural reactivation across two phases in the LOC affected subsequent memory in the schema-C condition. This is consistent with the view that cortical regions act as scaffolds to assimilate new information. In another study using RSA, famous faces induced assimilation of new information into old memories in the inferior frontal gyrus - a semantic-related cortical region (Bein et al. 2020). Here, we tested our hypothesis in the stimuli representational cortical regions (e.g., the LOC and PPA) related to our

schema manipulation. Those results suggest that the involvement of specific cortical regions may be connected to the particular schema to be encoded within (van Kesteren et al. 2012; McClelland 2013; McClelland et al. 2020), consistent with the theory that the expression of memory is accompanied by co-activation of its corresponding neural structure and vice-versa (Moscovitch et al. 2016; Sekeres et al. 2018).

In regard to the relationship between LOC reactivation and memory, one concern may be that both of the trials in this analysis contain the same object representation and thus the object representation itself could drive the fMRI pattern analysis results as well as the improved memory results. In other words, any kind of association with each object should lead to greater pattern similarity across those critical trials as well as better memory. Previous studies suggest that the LOC is related to categorical clustering (Eger et al. 2008) and the object representations in this region are also reactivated more easily to match the previously seen representations when object-based schema is consistent (van der Linden et al. 2017). Consistent with those literature, the results in this study show that the reactivation in LOC was related to subsequent memory only in schema-C condition. The reactivation of same object in schema-IC condition did not drive a subsequent memory effect. Therefore, the reactivation results are unlikely to be explained by the object representation itself. Moreover, it could be that stable representations of schema were formed in the LOC after the training in schema-C condition but not in the schema-IC condition, and thus helped the integration of new information.

Another concern is that the PAs in the schema-C condition were easier to learn during the training than in the schema-IC condition, resulting in more positively reward associated with these objects. This might also induce stronger within-grid similarity and greater reactivation. We therefore did a control analysis to investigate whether the similarity between two grids in the schema-C condition is higher than that in the schema-IC condition (Figure S4). There was no evidence that two schema-C grids shared higher similarity, which suggests that the schema are specific within each grid, at least in our selected ROIs (LOC). To explore this possibility, further studies with a similar paradigm could ask participants to rate how rewarding they found each object after the training.

Cortical reactivations might be influenced by whether novel information is consistent, inconsistent, or arbitrary with respect to existing schema. Although we manipulated schema as networks of object-location associations, our results were based on new arbitrary object-scene associations that were not directly related to the trained schemas. Reactivation provokes a state of memory instability that may lead to interference and forgetting (Hupbach 2011; Fernández et al. 2016), but it also provides an opportunity for memories to interact with one another (Robertson 2012). This allows more general aspects of memory to be integrated (Ferreira et al. 2019). Here, reactivation may depend on whether or not the encoding occurs in a stable schema context. This reactivation of schema could act as a scaffold to assimilate new information, even the new information is not directly related to the schema, i.e.,

‘method of loci’ (Martin Dresler et al. 2017). After three days of training, the participants not only formed a schema of object-location networks but also formed the schema of objects clustering based on the location information (e.g., the alarm clock is always next to the bin and the broom). During new learning, the reactivation could be part of the schema; for example, the stable representations of objects clustering such as ‘clock-bin-broom’ were reactivated automatically, which might explain why the LOC didn’t contain general grid-based information (within vs. across) in the new learning. In our daily life, the new information is not always totally consistent or inconsistent with our prior knowledge. Recent studies also indicate that schema can modulate memory for schema-irrelevant information (Webb and Dennis 2020; Cockcroft et al. 2022). Therefore, even if the new information is not directly related to the schema, a stable schema could still provide scaffold-like representations and induce a different route to encode/incorporate new information.

Regarding the classical theory of systems consolidation, recent findings suggest that independent cortical memory representations can emerge rapidly (Cowansage et al. 2014; Kitamura et al. 2017; Brodt et al. 2018). These early cortical engrams, however, are ‘silenced’ shortly after learning (Kitamura et al. 2017). In human studies, cortical representations emerge after the repeated retrieval of prior material (Brodt et al. 2018; Himmer et al. 2019). Repeated retrieval may help develop cortical engrams, which is similar to a schema manipulation in that it also requires multiple training/retrieval. In addition, Bein and colleagues (2020) also showed that semantic schema could induce

assimilation in the semantic-related cortical region. Along with our results showing cortical reactivation and connectivity during encoding and their relations to memory performance after 24 h, these findings suggest that on the one hand, regardless of whether there is parallel encoding of new information into both hippocampus and prefrontal cortex (Tse et al. 2007; 2011), schema or prior knowledge may also induce rapid learning directly in stimulus-relevant cortical regions (Hebscher et al. 2019). On the other hand, the vmPFC has been shown to be involved in the integration and updating of reactivated memory traces (Preston and Eichenbaum 2013; Gilboa and Marlatte 2017; Sommer 2017; Hebscher et al. 2019). In our study, activation of the vmPFC was also associated with subsequent associative memory. Thus, it could also be that the vmPFC meditated the schema-related cortical learning. In any case, our study provides novel evidence of stimulus-relevant cortical learning in addition to the vmPFC and hippocampus during schema-related memory formation.

This cortical learning may further require sleep in order to be consolidated (Himmer et al. 2019; de Sousa et al. 2019), which is consistent with our results showing that fMRI effects during encoding were related to memory 24 hour later. Neuroimaging studies have shown that the durability of memories is associated with the brain activity/representation during encoding (e.g., Sneve et al. 2015; Wagner et al. 2016; Wagner et al. 2019; Wagner et al. 2021; Ness et al. 2022). Therefore, in the schema-related memory formation, while schema might strengthen mnemonic representations at initial encoding, their effects are enhanced during subsequent consolidation (Lewis

and Durrant 2011; Hennies et al. 2016), as also suggested by van Kesteren et al (2012). The neural changes during encoding may further underlie the neural mechanisms of schema-related fast memory consolidation (Fernández and Morris 2018).

In conclusion, we found that activations in the vmPFC and anterior hippocampus were important for new schema-related integration. Further, object-based clustering of schematic information could be represented in the LOC in the retrieval of schema training information, but not in new associative encoding. However, the reactivation of representations in the LOC played a role in new associative encoding only in the schema-C condition, which may increase LOC–PPA cortical connectivity. Taken together, our findings shed further light on how schema reactivation in cortical regions supports the integration of novel information into existing memory networks, as a potential neural mechanism for schema-induced rapid learning.

Data availability statement

The data that support the findings of this study are not publicly available due to restrictions imposed by the administering institution and privacy of the participants. The authors will share them by request from any qualified investigator after completion of a data sharing agreement.

References

Alba JW, Hasher L. 1983. Is memory schematic? Psychol Bull. 93(2):203–231. doi:10.1037/0033-2909.93.2.203.

Alonso A, van der Meij J, Tse D, Genzel L. 2020. Naïve to expert: Considering the role of previous knowledge in memory. Brain Neurosci Adv. 4:2398212820948686.

Audrain S, McAndrews MP. 2022. Schemas provide a scaffold for neocortical integration of new memories over time. Nat Commun. 13(1):1–16.

Baldassano C, Hasson U, Norman KA. 2018. Representation of real-world event schemas during narrative perception. Journal of Neuroscience. 38(45):9689–9699.

Baraduc P, Duhamel J-R, Wirth S. 2019. Schema cells in the macaque hippocampus. Science (1979). 363(6427):635–639.

Bartlett FC. 1932. Remembering : A Study in Experimental and Social Psychology. Cambridge, Social Psychology. doi:10.1111/j.2044-8279.1933.tb02913.x.

Bein O, Reggev N, Maril A. 2014. Prior knowledge influences on hippocampus and medial prefrontal cortex interactions in subsequent memory. Neuropsychologia. 64:320–330. doi:10.1016/j.neuropsychologia.2014.09.046.

Bein O, Reggev N, Maril A. 2020. Prior knowledge promotes hippocampal separation but cortical assimilation in the left inferior frontal gyrus. Nat Commun. 11(1):1–13.

Bein O, Trzewik M, Maril A. 2019. The role of prior knowledge in incremental associative learning: An empirical and computational approach. J Mem Lang. 107:1–24.

Bonasia K, Sekeres MJ, Gilboa A, Grady CL, Winocur G, Moscovitch M. 2018. Prior knowledge modulates the neural substrates of encoding and retrieving naturalistic events at short and long delays. Neurobiol Learn Mem. 153(October 2017):26–39. doi:10.1016/j.nlm.2018.02.017.

Bracci S, de Beeck HO. 2016. Dissociations and associations between shape and category representations in the two visual pathways. Journal of Neuroscience. 36(2):432–444.

Brainard DH, Vision S. 1997. The psychophysics toolbox. Spat Vis. 10:433–436.

Bransford JD. 1979. Human cognition: Learning, understanding and remembering.

Brod G, Lindenberger U, Wagner AD, Shing YL. 2016. Knowledge Acquisition during Exam Preparation Improves Memory and Modulates Memory Formation. Journal of Neuroscience. 36(31):8103–8111. doi:10.1523/JNEUROSCI.0045-16.2016. http://www.jneurosci.org/cgi/doi/10.1523/JNEUROSCI.0045-16.2016.

Brodeur MB, Dion-Lessard G, Chauret M, Dionne-Dostie E, Montreuil T, Lepage M. 2010. The Bank of Standardized Stimuli (BOSS): a new normative dataset of 480 visual stimuli to be used in visual cognition research. PLoS One. 11(11).

Brodt S, Gais S, Beck J, Erb M, Scheffler K, Schönauer M. 2018. Fast track to the neocortex: A memory engram in the posterior parietal cortex. Science (1979). 362(6418):1045–1048.

van Buuren M, Kroes MCW, Wagner IC, Genzel L, Morris RGM, Fernandez G. 2014. Initial Investigation of the Effects of an Experimentally Learned Schema on Spatial Associative Memory in Humans. Journal of Neuroscience. 34(50):16662–16670. doi:10.1523/JNEUROSCI.2365-14.2014.

Cockcroft JP, Berens SC, Gaskell MG, Horner AJ. 2022. Schematic information influences memory and generalisation behaviour for schema-relevant and-irrelevant information. Cognition. 227:105203.

Cowansage KK, Shuman T, Dillingham BC, Chang A, Golshani P, Mayford M. 2014. Direct reactivation of a coherent neocortical memory of context. Neuron. 84(2):432–441.

Cox RW. 1996. AFNI: software for analysis and visualization of functional magnetic resonance neuroimages. Comput Biomed Res. 29(3):162–73. doi:10.1006/cbmr.1996.0014.

Danker JF, Anderson JR. 2010. The ghosts of brain states past: remembering reactivates the brain regions engaged during encoding. Psychol Bull. 136(1):87.

Eger E, Ashburner J, Haynes J-D, Dolan RJ, Rees G. 2008. fMRI activity patterns in human LOC carry information about object exemplars within category. J Cogn Neurosci. 20(2):356–370.

Epstein RA, Baker CI. 2019. Scene perception in the human brain. Annu Rev Vis Sci. 5:373.

Fernández G, Morris RGM. 2018. Memory, novelty and prior knowledge. Trends Neurosci. 41(10):654–659.

Fernández RS, Bavassi L, Kaczer L, Forcato C, Pedreira ME. 2016. Interference conditions of the reconsolidation process in humans: The role of valence and different memory systems. Front Hum Neurosci. 10:641.

Ferreira CS, Charest I, Wimber M. 2019. Retrieval aids the creation of a generalised memory trace and strengthens episode-unique information. Neuroimage. 201:115996.

Fischl B, Dale AM. 2000. Measuring the thickness of the human cerebral cortex from magnetic resonance images. Proceedings of the National Academy of Sciences. 97(20):11050–11055. doi:10.1073/pnas.200033797.

Gardiner JM, Ramponi C, Richardson-Klavehn A. 1998. Experiences of remembering, knowing, and guessing. Conscious Cogn. 7(1):1–26.

Gilboa A, Marlatte H. 2017. Neurobiology of Schemas and Schema-Mediated Memory. Trends Cogn Sci. 21(8):618–631. doi:10.1016/j.tics.2017.04.013.

Giuliano AE, Bonasia K, Ghosh VE, Moscovitch M, Gilboa A. 2021. Differential Influence of Ventromedial Prefrontal Cortex Lesions on Neural Representations of Schema and Semantic Category Knowledge. J Cogn Neurosci. 33(9):1928–1955.

Guo D, Yang J. 2020. Interplay of the long axis of the hippocampus and ventromedial prefrontal cortex in schema-related memory retrieval. Hippocampus. 30(3):263–277.

Hebscher M, Wing E, Ryan J, Gilboa A. 2019. Rapid cortical plasticity supports long-term memory formation. Trends Cogn Sci. 23(12):989–1002.

Hennies N, Ralph MAL, Kempkes M, Cousins JN, Lewis PA. 2016. Sleep spindle density predicts the effect of prior knowledge on memory consolidation. Journal of Neuroscience. 36(13):3799–3810.

Himmer L, Schönauer M, Heib DPJ, Schabus M, Gais S. 2019. Rehearsal initiates systems memory consolidation, sleep makes it last. Sci Adv. 5(4):eaav1695.

Hupbach A. 2011. The specific outcomes of reactivation-induced memory changes depend on the degree of competition between old and new information. Front Behav Neurosci. 5:33.

st. Jacques PL, Schacter DL. 2013. Modifying memory: Selectively enhancing and updating personal memories for a museum tour by reactivating them. Psychol Sci. 24(4):537–543.

van Kesteren MTR, Beul SF, Takashima A, Henson RN, Ruiter DJ, Fernández G. 2013. Differential roles for medial prefrontal and medial temporal cortices in schema-dependent encoding: From congruent to incongruent. Neuropsychologia. 51(12):2352–2359. doi:10.1016/j.neuropsychologia.2013.05.027.

van Kesteren Marlieke T R, Brown TI, Wagner AD. 2018. Learned spatial schemas and prospective hippocampal activity support navigation after one-shot learning. Front Hum Neurosci. 12:486.

van Kesteren MTR, Fernandez G, Norris DG, Hermans EJ. 2010. Persistent schema-dependent hippocampal-neocortical connectivity during memory encoding and postencoding rest in humans. Proceedings of the National Academy of Sciences. 107(16):7550–7555. doi:10.1073/pnas.0914892107.

van Kesteren Marlieke Tina Renée, Krabbendam L, Meeter M. 2018. Integrating educational knowledge: reactivation of prior knowledge during educational learning enhances memory integration. NPJ Sci Learn. 3(1):1–8.

van Kesteren MTR, Rignanese P, Gianferrara PG, Krabbendam L, Meeter M. 2020. Congruency and reactivation aid memory integration through reinstatement of prior knowledge. Sci Rep. 10(1):1–13.

van Kesteren MTR, Rijpkema M, Ruiter DJ, Morris RGM, Fernández G. 2014. Building on prior knowledge: schema-dependent encoding processes relate to academic performance. J Cogn Neurosci. doi:10.1162/jocn_a_00630.

van Kesteren Marlieke T.R., Ruiter DJ, Fernández G, Henson RN. 2012. How schema and novelty augment memory formation. Trends Neurosci. 35(4):211–219. doi:10.1016/j.tins.2012.02.001.

van Kesteren Marlieke T R, Ruiter DJ, Henson RN. 2012. How schema and novelty augment memory formation. :1–9. doi:10.1016/j.tins.2012.02.001.

Kitamura T, Ogawa SK, Roy DS, Okuyama T, Morrissey MD, Smith LM, Redondo RL, Tonegawa S. 2017. Engrams and circuits crucial for systems consolidation of a memory. Science (1979). 356(6333):73–78.

Kleiner M, Brainard D, Pelli D, Ingling A, Murray R, Broussard C, others. 2007. What's new in Psychtoolbox-3. Perception. 36(14):1.

Lewis PA, Durrant SJ. 2011. Overlapping memory replay during sleep builds cognitive schemata. Trends Cogn Sci. 15(8):343–351.

van der Linden M, Berkers RMWJ, Morris RGM, Fernández G. 2017. Angular gyrus involvement at encoding and retrieval is associated with durable but less specific memories. The Journal of Neuroscience.:3603–16. doi:10.1523/JNEUROSCI.3603-16.2017.

Liu ZX, Grady C, Moscovitch M. 2017. Effects of Prior-Knowledge on Brain Activation and Connectivity During Associative Memory Encoding. Cereb Cortex. 27(3):1991–2009. doi:10.1093/cercor/bhw047.

Liu ZX, Grady C, Moscovitch M. 2018. The effect of prior knowledge on post-encoding brain connectivity and its relation to subsequent memory. Neuroimage. 167(July 2017):211–223. doi:10.1016/j.neuroimage.2017.11.032.

Mackey S, Petrides M. 2014. Architecture and morphology of the human ventromedial prefrontal cortex. European Journal of Neuroscience. 40(5):2777–2796. doi:10.1111/ejn.12654.

Martin Dresler A, Shirer WR, Konrad BN, Ferná ndez G, Czisch M, Greicius Correspondence MD, Dresler M, M NC, Wagner IC, Greicius MD. 2017. Mnemonic Training Reshapes Brain Networks to Support Superior Memory Article Mnemonic Training Reshapes Brain Networks to Support Superior Memory. Neuron. 93(5):1227–1235. doi:10.1016/j.neuron.2017.02.003

Masís-Obando R, Norman KA, Baldassano C. 2021. Schema representations in distinct brain networks support narrative memory during encoding and retrieval. bioRxiv.

McClelland JL. 2013. Incorporating rapid neocortical learning of new schema-consistent information into complementary learning systems theory. J Exp Psychol Gen. 142(4):1190.

McClelland JL, McNaughton BL, Lampinen AK. 2020. Integration of new information in memory: new insights from a complementary learning systems perspective. Philosophical Transactions of the Royal Society B. 375(1799):20190637.

McKenzie S, Frank AJ, Kinsky NR, Porter B, Rivière PD, Eichenbaum H. 2014. Hippocampal representation of related and opposing memories develop within distinct, hierarchically organized neural schemas. Neuron. 83(1):202–215. doi:10.1016/j.neuron.2014.05.019.

Moreno-Martínez FJ, Montoro PR. 2012. An ecological alternative to Snodgrass & Vanderwart: 360 high quality colour images with norms for seven psycholinguistic variables. PLoS One. doi:10.1371/journal.pone.0037527.

Moscovitch M, Cabeza R, Winocur G, Nadel L. 2016. Episodic Memory and Beyond: The Hippocampus and Neocortex in Transformation. Annu Rev Psychol. 67(1):105–134. doi:10.1146/annurev-psych-113011-143733.

Mumford JA, Davis T, Poldrack RA. 2014. The impact of study design on pattern estimation for single-trial multivariate pattern analysis. Neuroimage. 103:130–138.

Mumford JA, Turner BO, Ashby FG, Poldrack RA. 2012. Deconvolving BOLD activation in event-related designs for multivoxel pattern classification analyses. Neuroimage. 59(3):2636–2643.

Ness HT, Folvik L, Sneve MH, Vidal-Piñeiro D, Raud L, Geier OM, Nyberg L, Walhovd KB, Fjell AM. 2022. Reduced Hippocampal-Striatal Interactions during Formation of Durable Episodic Memories in Aging. Cerebral Cortex. 32(11):2358–2372.

Nicolás B, Sala-Padró J, Cucurell D, Santurino M, Falip M, Fuentemilla L. 2021. Theta rhythm supports hippocampus-dependent integrative encoding in schematic/semantic memory networks. Neuroimage. 226:117558.

Nyberg L, Habib R, McIntosh AR, Tulving E. 2000. Reactivation of encoding-related brain activity during memory retrieval. Proceedings of the National Academy of Sciences. 97(20):11120–11124.

Pelli DG. 1997. The VideoToolbox software for visual psychophysics: Transforming numbers into movies. Spat Vis. 10(4):437–442.

Poppenk J, Evensmoen HR, Moscovitch M, Nadel L. 2013. Long-axis specialization of the human hippocampus. Trends Cogn Sci. 17(5):230–240. doi:10.1016/j.tics.2013.03.005.

Preston AR, Eichenbaum H. 2013. Interplay of hippocampus and prefrontal cortex in memory. Current Biology. 23(17):R764–R773. doi:10.1016/j.cub.2013.05.041.

Rajaram S. 1993. Remembering and knowing: Two means of access to the personal past. Mem Cognit. 21(1):89–102.

Rissman J, Gazzaley A, D'Esposito M. 2004. Measuring functional connectivity during distinct stages of a cognitive task. Neuroimage. 23(2):752–763.

Robertson EM. 2012. New insights in human memory interference and consolidation. Current Biology. 22(2):R66–R71.

Robin J, Moscovitch M. 2017. Details, gist and schema: hippocampal–neocortical interactions underlying recent and remote episodic and spatial memory. Curr Opin Behav Sci. 17:114–123. doi:10.1016/j.cobeha.2017.07.016.

Ryan JD, D'Angelo MC, Kacollja A, Gardner S, Rosenbaum RS. 2020. Gradual learning and inflexible strategy use in amnesia: Evidence from case HC. Neuropsychologia. 137:107280.

Schlichting ML, Mumford JA, Preston AR. 2015. Learning-related representational changes reveal dissociable integration and separation signatures in the hippocampus and prefrontal cortex. Nat Commun. 6(1):1–10.

Schlichting ML, Zeithamova D, Preston AR. 2014. CA1 subfield contributions to memory integration and inference. Hippocampus. 24(10):1248–1260.

Sekeres MJ, Winocur G, Moscovitch M. 2018. The hippocampus and related neocortical structures in memory transformation. Neurosci Lett. doi:10.1016/j.neulet.2018.05.006.

Skotko BG, Kensinger EA, Locascio JJ, Einstein G, Rubin DC, Tupler LA, Krendl A, Corkin S. 2004. Puzzling Thoughts for H . M .: Can New Semantic Information Be Anchored to Old Semantic Memories ? 18(4):756–769. doi:10.1037/0894-4105.18.4.756.

Sneve MH, Grydeland H, Nyberg L, Bowles B, Amlien IK, Langnes E, Walhovd KB, Fjell AM. 2015. Mechanisms underlying encoding of short-lived versus durable episodic memories. Journal of Neuroscience. 35(13):5202–5212.

Sommer T. 2017. The emergence of knowledge and how it supports the memory for novel related information. Cerebral Cortex. 27(3):1906–1921.

de Sousa AF, Cowansage KK, Zutshi I, Cardozo LM, Yoo EJ, Leutgeb S, Mayford M. 2019. Optogenetic reactivation of memory ensembles in the retrosplenial cortex induces systems consolidation. Proceedings of the National Academy of Sciences. 116(17):8576–8581.

Tompary A, Thompson-Schill SL. 2021. Semantic influences on episodic memory distortions. J Exp Psychol Gen.

Tse D, Langston RF, Kakeyama M, Bethus I, Spooner PA, Wood ER, Witter MP, Morris RGM. 2007. Schemas and memory consolidation. Science (1979). 316(5821):76–82. doi:10.1126/science.1135935.

Tse D, Takeuchi T, Kakeyama M, Kajii Y, Okuno H, Tohyama C, Bito H, Morris RGM. 2011. Schema-dependent gene activation and memory encoding in neocortex. Science (1979). 333(6044):891–895. doi:10.1126/science.1205274.

Tulving E, Thomson DM. 1973. Encoding specificity and retrieval processes in episodic memory. Psychol Rev. 80(5):352.

Wagner IC, van Buuren M, Bovy L, Fernández G. 2016. Parallel engagement of regions associated with encoding and later retrieval forms durable memories. Journal of Neuroscience. 36(30):7985–7995.

Wagner IC, van Buuren M, Fernández G. 2019. Thalamo-cortical coupling during encoding and consolidation is linked to durable memory formation. Neuroimage. 197:80–92.

Wagner IC, Konrad BN, Schuster P, Weisig S, Repantis D, Ohla K, Kühn S, Fernández G, Steiger A, Lamm C. 2021. Durable memories and efficient neural coding through mnemonic training using the method of loci. Sci Adv. 7(10):eabc7606.

Webb CE, Dennis NA. 2020. Memory for the usual: the influence of schemas on memory for non-schematic information in younger and older adults. Cogn Neuropsychol. 37(1–2):58–74.

Webb CE, Turney IC, Dennis NA. 2016. What's the gist? The influence of schemas on the neural correlates underlying true and false memories. Neuropsychologia. 93(July):61–75. doi:10.1016/j.neuropsychologia.2016.09.023.

Yonelinas AP. 2002. The nature of recollection and familiarity: A review of 30 years of research. J Mem Lang. 46(3):441–517.

Yousuf M, Packard PA, Fuentemilla L, Bunzeck N. 2021. Functional coupling between CA3 and laterobasal amygdala supports schema dependent memory formation. Neuroimage. 244:118563.

Zeithamova D, Dominick AL, Preston AR. 2012. Hippocampal and ventral medial prefrontal activation during retrieval-mediated learning supports novel inference. Neuron. 75(1):168–179. doi:10.1016/j.neuron.2012.05.010.

Zeithamova D, Preston AR. 2010. Flexible memories: differential roles for medial temporal lobe and prefrontal cortex in cross-episode binding. Journal of Neuroscience. 30(44):14676–14684.

Zhan L, Guo D, Chen G, Yang J. 2018. Effects of repetition learning on associative recognition over time: Role of the hippocampus and prefrontal cortex. Front Hum Neurosci. 12. doi:10.3389/fnhum.2018.00277.

Zheng L, Gao Z, McAvan AS, Isham EA, Ekstrom AD. 2021. Partially overlapping spatial environments trigger reinstatement in hippocampus and schema representations in prefrontal cortex. Nat Commun. 12(1):1–15.

Zhou J, Jia C, Montesinos-Cartagena M, Gardner MPH, Zong W, Schoenbaum G. 2021. Evolving schema representations in orbitofrontal ensembles during learning. Nature. 590(7847):606–611.